



Cite this: *Chem. Commun.*, 2015, 51, 7781

Supramolecular electron transfer-based switching involving pyrrolic macrocycles. A new approach to sensor development?

Nathan L. Bill,^a Olga Trukhina,^{ab} Jonathan L. Sessler^{*c} and Tomás Torres^{*ab}

This Feature focuses on pyrrolic macrocycles that can serve as switches *via* energy- or electron transfer (ET) mechanisms. Macrocycles operating by both ground state (thermodynamic) and photoinduced ET pathways are reviewed and their ability to serve as the readout motif for molecular sensors is discussed. The aim of this article is to highlight the potential utility of ET in the design of systems that perform molecular switching or logic functions and their applicability in chemical sensor development. The conceptual benefits of this paradigm are illustrated with examples drawn mostly from the authors' laboratories.

Received 21st December 2014,
Accepted 20th February 2015

DOI: 10.1039/c4cc10193f

www.rsc.org/chemcomm

1. Introduction

The development of molecular sensors capable of detecting and quantifying the presence of chemically or biologically important analytes is a topic of considerable current interest. Typically, molecular sensors contain a readout element, which *detectibly* and *reversibly* changes the state of the system upon interaction

with an analyte of interest. To date, a wide variety of systems that rely on changes in the absorptive,¹ emissive,^{1,2} structural,³ or redox properties⁴ of the readout element have been reported. Other systems, including polymers,⁵ multi-component arrays,⁶ and solid supported devices,⁷ that act as molecular switches or logic devices have also been exploited for the purpose of chemical sensing. However, the development of new modalities that might allow for the detection of analytes is of vital importance for the progression of the recognition, sensing, and molecular logic device fields.

Recently, we, among others, have become interested in studying non-covalent energy- and electron transfer processes and analyzing how the underlying interactions vary as a function of environment.^{8–11} Classically, energy- and electron transfer interactions can be divided into redox processes (full change in

^a Departamento de Química Orgánica, Facultad de Ciencias, Universidad Autónoma de Madrid, Cantoblanco, 28049-Madrid, Spain. E-mail: tomas.torres@uam.es

^b IMDEA-Nanociencia, 28049-Madrid, Spain

^c Department of Chemistry, The University of Texas at Austin, 105 East 24th Street-Stop A5300, Austin, Texas 78712-1224, USA. E-mail: sessler@cm.utexas.edu



Nathan L. Bill

Nathan Bill was a student athlete (soccer) at Central College, where he received a BA in Chemistry in 2007. He then commenced his graduate studies at the University of Texas at Austin under the tutelage of Prof. Jonathan Sessler. In 2013, he received his PhD defending his dissertation entitled "Extension of Tetrathiafulvalene Conjugation Through Pyrrolic-Based Dyes: ExTTF Porphyrin and ExTTF BODIPY." Currently, he is a Marie Curie International

Incoming Fellow at Universidad Autónoma de Madrid, working in the group of Prof. Tomás Torres.



Olga Trukhina

Olga Trukhina graduated from the Ivanovo State University of Chemistry and Technology, Russia, in 2007 and then became a PhD student under the guidance of Prof. Mikhail K. Islyaikin and Prof. Tomás Torres, working on expanded porphyrin aza-analogues. In 2010, she started working in the synthesis of phthalocyanine-based molecular nanosystems as a fellow within the group of Prof. Torres and continues her research under his guidance at the IMDEA-Nanoscience.

oxidation states of the components), charge transfer complexes (partial charge transfer as a result of favorable orbital overlap between the constituent donors and acceptors), and photo-induced energy- or electron transfer (*i.e.*, charge transfer stimulated by spectroelectrical illumination). A vast and continually increasing amount of research effort has been devoted to systems displaying these features, driven by the widespread interest in molecular electronic devices, photosynthetic mimics, and photocatalysis. However, in spite of the ubiquity of energy- and electron transfer processes and their obvious importance in a range of areas, both fundamental and applied, little work has been devoted to exploiting the underlying interactions as the basis for sensor development.

In this Feature we aim to highlight oligopyrrole-based charge transfer systems that have the potential to be applied as molecular sensors. Particular focus will be placed on systems where the addition of an outside stimulus or analyte leads to a *thermodynamic electron transfer* (ET) event being turned on, off, or in some cases reversed. Examples involving supramolecular ET systems, in which the donor and acceptor are linked *via* supramolecular interactions, will receive the greatest emphasis. Such systems are expected to be inherently more useful, and more sensitive, when applied as sensors since changes in the key supramolecular associations can serve to alter the spatial configuration of the system and thus the rate of ET between the electroactive donor-acceptor components. While there are a number of systems that might potentially be considered as non-covalent, ET-based sensor systems, to limit the number of examples, this Feature will concentrate on analyte-dependent, energy- and electron transfer ensembles involving pyrrolic macrocycles. Other than considerations of length, the justification for targeting this class of molecules is multifaceted.

Specifically, such macrocycles are (1) well-studied with countless examples having been reported in the literature, (2) easily modified *via* synthetically modification or metalation of the central core, (3) can be tuned to emit and absorb light throughout the visible and NIR spectrum, (4) form stable and well-defined radical cations and anions upon oxidation and reduction, respectively, and (5) have been shown to form supramolecular complexes though axial metal coordination, as well as electrostatic, π - π donor-acceptor, van der Waals, and hydrogen bonding interactions.¹² Our goal in writing this Feature is to show how appropriately chosen constructs containing pyrrolic macrocycles can be considered as analyte-dependent electron transfer switches and thus as a new class of molecular sensors. It is hoped that this will serve to set the stage for future developments in the field.

2. Dynamics of electron transfer (Marcus theory)

Electron transfer reactions, often referred to as redox reactions, consist of the transfer of an electron from one species (donor or reductant) to another species (acceptor or oxidant). Between discrete molecules, such ET events occur through one of two limiting pathways: inner sphere or outer sphere. In the inner sphere mechanism, the donor and acceptor are bridged during the electron transfer process, resulting in large changes to the coordination sphere of the products compared to the reactants, including alterations in the number, type, and lengths of bonds or the ligands surrounding the redox center. In outer sphere electron transfer reactions no bonds are formed or broken. Instead, upon close contact of the redox active species *via e.g.*, diffusion or supramolecular complexation, an electron “hops”



Jonathan L. Sessler

Prof. Jonathan L. Sessler received a BS degree (with Highest Honors) in chemistry in 1977 from the University of California, Berkeley and a PhD in organic chemistry from Stanford University in 1982 (supervisor: Professor James P. Collman). After completing NSF-CNRS and NSF-NATO Post-doctoral Fellowships with Professor Jean-Marie Lehn at L'Université Louis Pasteur de Strasbourg, France, he was a JSPS Visiting Scientist in Professor Tabushi's

group in Kyoto, Japan. In September 1984, he accepted a position as an Assistant Professor of Chemistry at the University of Texas at Austin, where he is currently the Roland K. Pettit Chair. To date, Dr Sessler has published over 600 independent research publications, coauthored two books, and been an inventor of record on almost 80 issued US Patents. Dr Sessler is a co-founder of Pharmacyclics, Inc., a publicly traded company (pcyc; NASDAQ) dedicated to developing new cancer therapies.



Tomás Torres

Tomás Torres is Full Professor of Organic Chemistry at the Autónoma University of Madrid (UAM) and Associated Senior Scientist at the IMDEA-Nanoscience. In addition to various aspects of synthetic and supramolecular chemistry, his current research interests include the preparation and study of optical properties of organic functional materials. His group, that presently consists of twenty five researchers, is currently exploring several areas of basic

research and applications of phthalocyanines, porphyrins and carbon nanostructures (fullerenes, carbon nanotubes, graphene), including organic and hybrid solar cells, with a focus on nanotechnology.

through space (tunnels) from the donor to the acceptor completing the ET process. Typically, outer sphere ET processes are preferred when the rate of electron transfer is faster than ligand substitution, when there are no suitable bridging ligands, or when one or both of the electroactive components is inert. Thus, for supramolecular switching applications, the outer sphere mechanism is of greater interest.

A number of rate expressions have been introduced to the literature that may be used to predict whether an outer shell ET reaction will take place in the forward or back directions and whether the resulting charge separated (CS) state will be stable. Of these, the "Marcus Theory", pioneered by Rudolf A. Marcus (for which he received the Nobel Prize in Chemistry in 1992), is the best known.¹³ It relies on a transition-state theoretical approach and is accessible to the non-specialist. Unlike classical reaction mechanisms (such as S_N2) subject to microscopic reversibility, in ET, the electron undergoing reaction is quantized. It resides either fully on the donor or fully on the acceptor. Thus, the solvent and solvation state have enhanced importance. Specifically, the movement of electrons from donor to acceptor happens on a much faster time scale than the reorganization of large solvent molecules. Therefore, and according to the Franck-Condon principle,¹⁴ the nuclear orientations of the reactants, products, and the solvent, must be degenerate. In other words their orientations must be identical before and after the electron "jumps." However, since energy must also be conserved during the ET process for any non-isoergic reaction, the solvent sphere of the reactants and the products cannot be the same; rather, its orientation must lie somewhere in between the two. Consequently, the energy required to reorganize the solvent shell into a state where ET can occur (corresponding to the hypothetical transfer of a partial electron) is equivalent to the activation barrier, ΔG^\ddagger , of the ET reaction.

Marcus found that he could treat the complicated reaction coordinate diagram containing all of the coordinates for each individual solvent molecule within a single coordinate, the solvent polarization (P or Δe).¹⁵ Using eqn (1), the Gibbs free energy of the system becomes a function of Δe , where r_D and r_A are the radius of the donor and acceptor, respectively, R_{DA} is the distance between the donor and acceptor, and ϵ_{op} and ϵ_s are the optical and static dielectric constants of the solvent, respectively. The physical meaning of Δe in this equation is equivalent to the amount of charge transferred from the donor to the acceptor.

$$G = \left(\frac{1}{2r_D} + \frac{1}{2r_A} - \frac{1}{R_{DA}} \right) \cdot \left(\frac{1}{\epsilon_{op}} - \frac{1}{\epsilon_s} \right) \cdot (\Delta e)^2 \quad (1)$$

Plots of eqn (1) are parabolic in nature, and represent the amount of energy required to perturb the solvent environment of a system to that of an arbitrary amount of transferred charge. Although for any given ET event the amount of charge is quantized, the perturbation of the solvent is not, and can be treated classically. Thus, plotting eqn (1) for both the precursor (D and A) and successor ($D^{\bullet+}$ and $A^{\bullet-}$) complexes on the same axis allows a semi-quantitative understanding of the ET process (Fig. 1). For instance, the point where the parabolas intersect corresponds to the activation energy (ΔG^\ddagger) of the electron transfer process. Solving for this point (eqn (2)), Marcus found

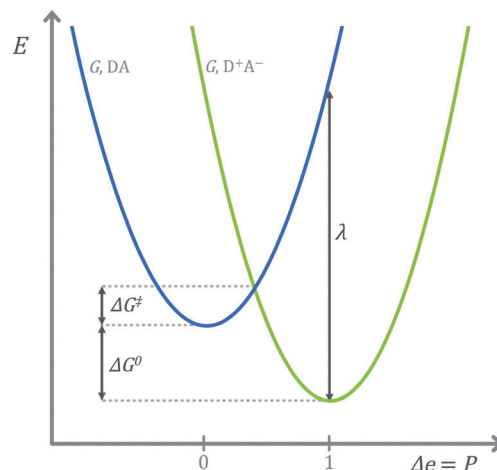


Fig. 1 Schematic diagram according to Marcus theory showing the parabolic outer sphere reorganization energies for a general donor-acceptor ET system. The first parabola (G, DA in blue) denotes the solvent polarization condition before the ET event while the second (G, D^+A^- in green) corresponds to the post ET situation. ΔG^\ddagger , ΔG^0 , and λ depict the activation energy, the free energy driving force, and the outer shell reorganization energy of the ET event, respectively.

ΔG^\ddagger as a function of the reorganization energy, λ_0 (the value of G in eqn (1) when $\Delta e = 1$) and the driving force, ΔG^0 , of the reaction.

$$\Delta G^\ddagger = \frac{(\lambda_0 + \Delta G^0)^2}{4\lambda_0} \quad (2)$$

Finally, substituting the activation energy into the Arrhenius equation, the rate constant is obtained (eqn (3)):

$$k = Ae^{-\frac{(\Delta G^0 + \lambda_0)^2}{4\lambda_0 RT}} \quad (3)$$

where A is a pre-exponential factor dependent on the distance between the redox pair, and the damping factor, R is the ideal gas constant, and T is the temperature of the solution.

A further peculiarity of Marcus theory is the so-called Marcus "inverted" region.¹⁶ In the "normal" region associated with Marcus theory, an increase in the free energy driving force, ΔG^0 , results in a decrease of the activation energy, ΔG^\ddagger (Fig. 2). This trend continues until $\Delta G^\ddagger = 0$, or in other words, the point in which an electron can be transferred from the precursor to the successor complex without requiring the manipulation of the solvent environment of the precursor complex. At this value of ΔG^0 , the rate of electron transfer is at a maximum and approaches diffusion limits. However, further increasing the driving force leads to an increase in the activation barrier, ΔG^\ddagger , and a retardation of the reaction rates. This portion is termed the "inverted" region in Marcus theory and upon experimental confirmation,¹⁷ became one of the hallmarks of ET theory.

This brief discussion of the dynamics of electron transfer is included to illustrate the elementary theory behind ET processes and to serve as a starting point for design considerations of potential ET sensors. For a compound to serve efficiently as an ET sensor the shape and/or location of its parabolic Δe vs. G

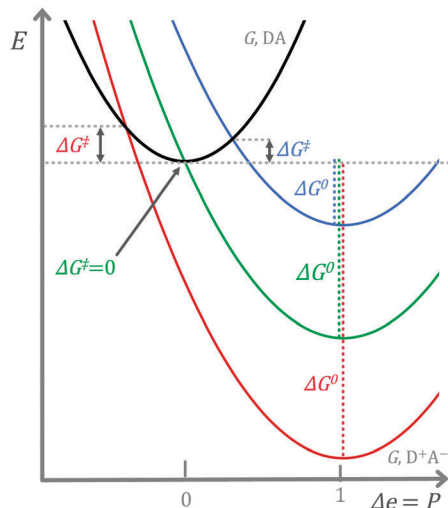


Fig. 2 Schematic diagram according to Marcus theory showing the effect of increasing the thermodynamic driving force ΔG^0 on the activation energy ΔG^\ddagger . Increasing ΔG^0 (going from the blue to the green successor parabola) leads to a concurrent decrease in ΔG^\ddagger , until $\Delta G^\ddagger = 0$. Subsequent increases of ΔG (from the green to red parabola) leads to an increase in the value ΔG^\ddagger . The latter transformation depicts the so-called "inverted" region of Marcus theory.

curve must be modified in a reversible (and ideally specific) manner upon exposure to an analyte. Thus, modifying the solvation sphere, reorganizational energy, Gibbs free energy of the donor or acceptor, or the distance between the donor and acceptor should have an effect on the rate of ET. These design principles provide a framework for the ensuing discussion of recent developments in the area.

3. Ground state ET systems

3.1 Biological systems

ET reactions are essential to the formation of energy rich chemicals (such as adenosine triphosphate (ATP)) that serve as the "molecular foods" for biological life. The two most important energy transductions in the biosphere – oxidative phosphorylation and photophosphorylation – together account for the vast majority of adenosine triphosphate (ATP) synthesized by aerobic organisms.¹⁸ The ET pathway for these processes involves the flow of electrons through a chain of redox intermediates including pyrrolic macrocycles (e.g., cytochromes), membrane-bound quinones, nicotinamide adenine dinucleotides, and other proteins. Further, these phosphorylation pathways are toggled on and off by transmembrane differences in ion concentrations and thus, can be considered as biological examples of supramolecular ET switches. Therefore, a brief review of selected natural pyrrole-based ET complexes is appropriate prior to discussing synthetic ET switching systems.

A canonical example of ground state ET within biological systems involves the transfer of electrons by *cytochrome c* (Cc) to *cytochrome c oxidase* (CcO). After receiving an electron from *cytochrome bc₁* complex the water-soluble heme protein Cc transfers electrons to the membrane bound heme-copper oxidase

CcO in the ultimate step of respiration. Minimal structural changes occur within Cc upon switching between its oxidized (Fe^{3+}) and reduced (Fe^{2+}) forms, maintaining the near-planarity of the heme molecule during phosphorylation.¹⁹ The small structural changes in Cc and the unique solvent environments in the protein complexes most likely reduce the reorganizational energy between the oxidized and reduced forms, promoting rapid and efficient ground state ET. Further, the positively charged Cc and CcO proteins have been known to bind anions with varying affinities, inducing a redox-dependent structural change that alters the ET process.²⁰ Thus, ET reactions of cytochromes provide a proof-of-concept illustration that ET pathways can be promoted or inhibited by simple co-factors. Effectively, these prosthetic groups act as sensors for a key biological ET event.

3.2 Intermolecular ET systems

3.2.1 Tetrathiafulvalene calix[4]pyrrole. Inspired by the biological ET systems mentioned above, we attempted to achieve control over ET within synthetic supramolecular ensembles through the judicious addition of anions and cations. As detailed below, we found that by using a mixture of the electron donating tetrathiafulvalene-appended calix[4]pyrrole (TTF-C4P)²¹ with the dicationic electron acceptor bisimidazolium quinone (BIQ^{2+})²² we could reversibly switch the direction of electron transfer by varying the surrounding ionic environment.²³

Calix[4]pyrroles (C4P), in general, are a class of fluxional tetrapyrrolic macrocycles that bind selected anionic guests in organic solvents.^{4c,24} Upon anion complexation, a change in the conformation of the C4P macrocycle occurs, converting it from the so-called 1,3-alternate to the corresponding cone conformation. This flip in the stereochemical arrangement upon anion recognition is a result of the favorable and concerted hydrogen bonding interactions between the C4P pyrrolic N-H protons and the anionic guest, which are enhanced in the cone conformer. Upon C4P cone formation a bowl-like arrangement of the pyrrolic subunits is stabilized, into which appropriately sized cations have been shown to bind.²⁵

In the case of TTF-C4P, similar anion binding events and conformational changes occur, albeit with diminished anion affinities that are ascribed to the relatively electron rich nature of the tetrathiafulvalene moieties that serve to reduce the H-bond donor strength of the pyrrole rings.²⁶ As with simple C4Ps, conversion of TTF-C4P to its cone conformation serves to stabilize an electron rich bowl-shaped pocket that is able to accommodate large electron deficient guests, such as C_{60} .

Although charge transfer bands are seen when TTF-C4P and C_{60} are combined in the presence of an organic soluble chloride anion source, the fullerene is not a strong enough electron acceptor to induce ground state (thermodynamic) ET. It was hypothesized, however, that TTF-C4P in its anion-bound cone conformation could interact with a stronger electron acceptor to provide an ion-switchable ET ensemble.

This concept was confirmed experimentally by employing a bisimidazolium quinone (BIQ^{2+}) acceptor as a bis-cationic guest for TTF-C4P (Fig. 3). BIQ^{2+} was chosen for its large size, precluding any binding in the 1,3-alternate state of TTF-C4P, as

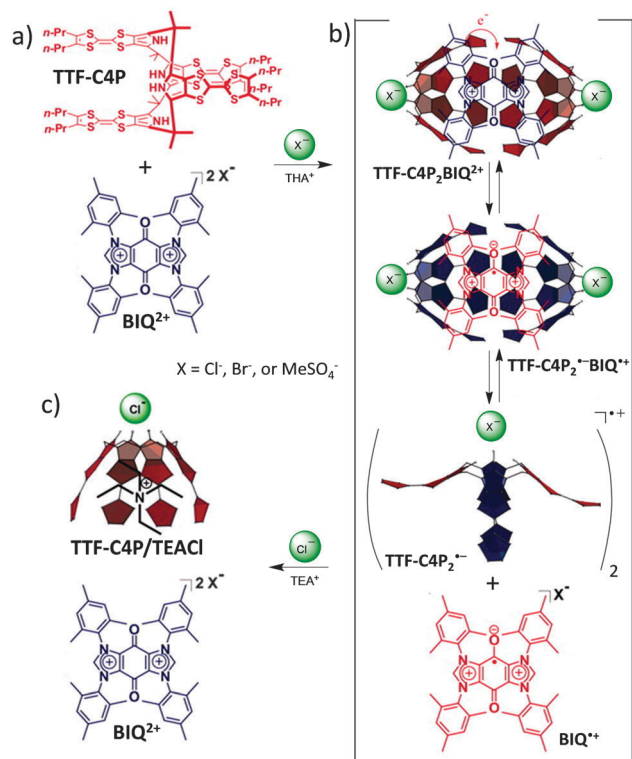


Fig. 3 Chemical structures of TTF-C4P and BIQ²⁺ (a) before the addition of any salts, (b) after the addition of THA⁺X⁻, where X = Cl⁻, Br⁻, or MeSO₄⁻, leading to an equilibrium between the complexed and uncomplexed states, and (c) after the addition of tetraethylammonium chloride, promoting back electron transfer.

well as for the fact that its first reduction wave is nearly isoenergetic with the first oxidation wave of TTF-C4P. Additionally, the counter anions of BIQ²⁺ could be varied. This, it was thought, would allow an ET event to be turned on (*i.e.*, stabilized in the forward TTF-C4P → BIQ²⁺ direction) by using a coordinating anion, such as Cl⁻, Br⁻, or MeSO₄⁻. In contrast, no ET was expected when a non-coordinating anion (BF₄⁻ or PF₆⁻) was employed.

When coordinating anions were employed as the BIQ²⁺ counteranions, strong changes in the absorption spectra were observed upon addition of the dicationic salt to TTF-C4P. Specifically, a band centered around *ca.* 750 nm and a very broad NIR feature extending from 1200 nm to over 2500 nm were found to increase and in a concentration-dependent manner. On the basis of comparison experiments involving direct chemical or electrochemical oxidation, the observed spectral features were ascribed to the radical cationic species (TTF-C4P)₂^{•+}. This was taken as evidence of ET being switched on.

Further evidence for ground state ET was obtained *via* electron paramagnetic resonance (EPR) spectroscopy. Two radical species, corresponding to TTF-C4P^{•+} (*g* = 2.0083) and BIQ^{•+} (*g* = 2.0056) were observed. These signals coincide with those obtained during independent EPR analysis of the chemical oxidation of TTF-C4P and electrochemical reduction of BIQ²⁺, respectively. It was therefore inferred that after ET, the coupled radical cationic complex (TTF-C4P)₂^{•+}·BIQ^{•+} dissociates into the constituent radical species TTF-C4P^{•+} and BIQ^{•+} (most likely due to electrostatic repulsion).

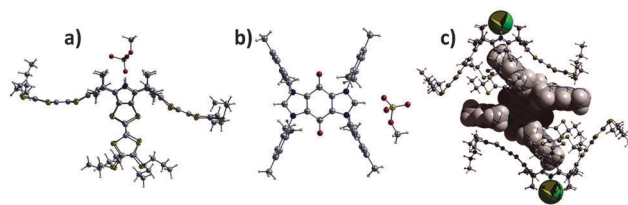


Fig. 4 Single crystal X-ray diffraction structures of (a) TTF-C4P^{•+}MeSO₄⁻, (b) BIQ^{•+}MeSO₄⁻ and (c) [TTF-C4P]₂^{•+}·[BIQ]^{•+}·2Cl⁻.

X-ray diffraction structures based on crystals grown from the mixture of TTF-C4P and BIQ²⁺·2MeSO₄⁻ gave additional support for the ET process. Upon slow diffusion of hexanes into a chloroform solution of TTF-C4P and BIQ²⁺·2MeSO₄⁻ a mixture of three different crystal types was formed. Separation of the sets of crystals by Pasteur's method and characterization by X-ray diffraction analysis yielded structures for TTF-C4P^{•+}MeSO₄⁻ and BIQ^{•+}MeSO₄⁻, and the complex (TTF-C4P)₂^{•+}·BIQ^{•+}·2MeSO₄⁻ (Fig. 4). These structural studies provided unequivocal solid state evidence for the proposed ET products, while providing strong support for the notion that ET occurs in solution as the result of complex formation.

In contrast to above, when salts of BIQ²⁺ containing counter anions that do not form complexes with TTF-C4P (and not triggering conversion of C4P from its 1,3-alternate to cone form) no ET was observed as inferred from UV-vis absorption and EPR spectroscopy or X-ray diffraction analyses. However, upon the addition of a coordinating ion source (*e.g.*, tetrahexylammonium chloride), to a mixture of TTF-C4P and either BIQ²⁺·2BF₄⁻ or BIQ²⁺·2PF₆⁻ (both being salts of non-coordinating anions), the characteristic absorption bands ascribed to the radical cationic (TTF-C4P)₂^{•+} species emerges. Such findings and associated EPR analyses, lend support to the conclusion that thermodynamic ET from TTF-CFP to BIQ²⁺ is only possible in the cone conformation. *Ipso facto*, a mixture of TTF-C4P and BIQ²⁺ serves as a rudimentary sensor for the Cl⁻, Br⁻, and MeSO₄⁻ anions. With them, ET occurs; without them, it does not.

An additional facet of the TTF-C4P-BIQ²⁺ system is that an alternative mode of ET control may be realized *via* competitive displacement of the BIQ²⁺ moiety. As noted above, the bowl-shaped cavity that is an intimate feature of the cone conformation of C4Ps will interact with cations. Similar effects are observed in the case of TTF-C4P, with the strength of cation binding interaction being strongly dependent on the size and charge density of the cationic guest. Tetra(ethyl, butyl, and hexyl)-ammonium cations (TEA⁺, TBA⁺, and THA⁺) were tested with TTF-C4P to evaluate the size-dependence of binding. The binding affinities were found to correlate inversely with the size of the cationic guest (*i.e.*, TEA⁺ > TBA⁺ > THA⁺). Further, addition of the smaller cationic guests was found to inhibit efficiently the forward ET process between TTF-C4P and BIQ²⁺. Specifically, titration of TEACl into a mixture of TTF-C4P and BIQ²⁺ (in chloroform) for which ET had been triggered *via* the use of a coordinating anion led to regeneration of the original absorption spectrum corresponding to TTF-C4P, as well as the near-elimination of the radical signals seen in the EPR

spectrum of the corresponding mixture based on THACl. Upon simply washing the system with water to enforce removal of the cationic tetraethylammonium salt, the ET state of the system was restored as inferred from color changes of the solution as well as spectroscopic analyses. Thus, in addition to being considered as an ET-based anion sensor the combined TTF-C4P-BIQ²⁺ ensemble may be used for cation identification, *i.e.*, allowing TEA⁺ to be distinguished from THA⁺.

In follow-up work, the BIQ²⁺ component in the aforementioned donor-acceptor ensembles was replaced by an endohedral fullerene, specifically Li⁺@C₆₀ (Fig. 5a).²⁷ Although previous studies had revealed interactions between TTF-C4P (in its cone conformation) and pristine C₆₀,²⁶ there was no evidence of actual ET occurring, as noted above. Li⁺@C₆₀,²⁸ on the other hand, is a much stronger acceptor (possessing a *ca.* 0.57 V cathodically shifted first reduction potential relative to C₆₀). Accordingly, Li⁺@C₆₀ was studied in the presence of TTF-C4P in benzonitrile solutions. In analogy to what was seen for the original TTF-C4P-BIQ²⁺ system, no electron transfer is observed between TTF-C4P and Li⁺@C₆₀ in the absence of a coordinating anion, presumably due to the predominant presence of the 1,3-alternate form of the putative TTF-C4P electron donor. Upon the addition of a coordinating anion source (*e.g.*, THACl), conversion to the cone conformation occurs and ground state ET is switched on, as substantiated by both absorption spectroscopy and EPR titrations (Fig. 5b and c).

The lack of broad NIR bands in the absorption spectrum and the hyperfine splitting pattern observed in the EPR spectrum (Fig. 5c) was taken as evidence that the oxidized TTF-C4P and reduced Li⁺@C₆₀ remain tightly coupled after ET. This stands

in contrast to the corresponding TTF-C4P-BIQ²⁺ system. The lack of NIR bands seen in the case of Li⁺@C₆₀ was considered indicative that the radical cation residing on the TTF-C4P is localized on one of the four TTF moieties, instead of being stabilized by neighboring TTF groups (which would result in mixed valence (NIR) bands). Most likely the overall neutral compound Li⁺@C₆₀^{•−} has the propensity to remain in the cup-shaped pocket of TTF-C4P^{•+} due to reduced electrostatic repulsion compared to the BIQ²⁺ system. Evidence for the formation of the presumed Cl[−]·TTF-C4P^{•+}Li⁺@C₆₀^{•−} ET complex came from a solid-state single crystal structural analysis. As was observed in the case of the BIQ²⁺ system, displacement of the endohedral fullerene from the cup with TEA⁺ salts led to reversal of the ET process.

3.2.2 Quinoidal π -extended tetrathiafulvalene porphyrins.

An alternative system recently reported by our group utilizes metal-ligand coordination bonds to control selectively the thermodynamic ET process. Quinoidal π -extended TTF porphyrins (MTTFP) (Fig. 6) were synthesized, metalated, and their redox characteristics studied.²⁹ In analogy to what has been observed for other π -extended TTF (ExtTTF) systems,³⁰ the MTTFPs were found to undergo a single two-electron oxidation (as opposed to two successive one-electron oxidations) at mild potentials as judged from cyclic voltammetric (CV) studies. These electrochemical features were ascribed to a combination of relatively reduced electrostatic repulsion in the dioxidized state (originating from the physically separated dithiolide rings) and the increase in stability resulting from aromatization of the central porphyrin core upon removal of a second electron.

Although only one two-electron oxidation wave was observed in the CV studies, subjecting MTTFPs to chemical oxidation using less than one molar equivalent of oxidant led to a stable radical cation intermediate (MTTFP^{•+}), which was characterized by both absorption and EPR spectroscopy. In these studies, tris(4-bromophenyl)-aminium hexachloro-antimonate (so called “magic blue”) was used as the oxidant. Further oxidation with magic blue led to the disappearance of the EPR signals and variations in the absorption spectra that were ascribed to the formation of the radical-free dicationic product, MTTFP²⁺. Thus, three oxidation states could be accessed in the case of the MTTFPs.

Modification of the central metal bound to the porphyrinoid core induces shifts in the oxidation potential in accord with the following trend: H₂ ≥ Ni > Cu > Zn. In fact, the oxidation wave of the metalated complex, ZnMTTFP, is shifted anodically

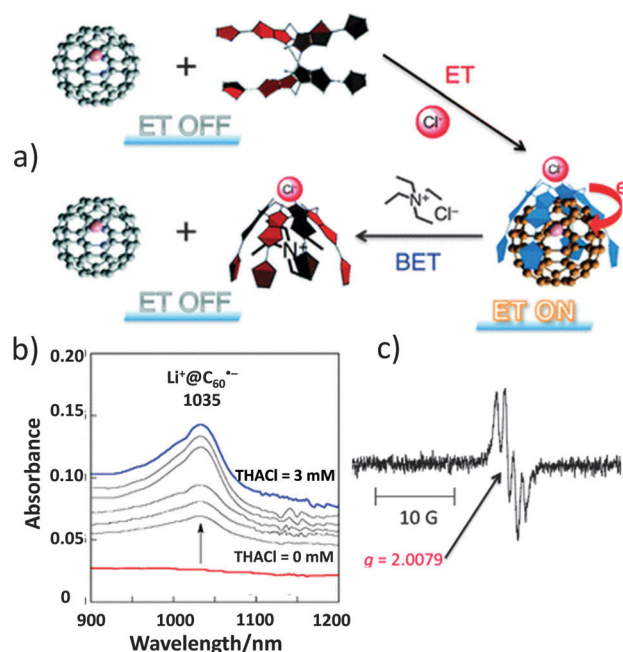


Fig. 5 (a) Proposed ion-controlled ET scheme between TTF-C4P and Li⁺@C₆₀. (b) NIR absorption spectral changes that are ascribed to the formation of Li⁺@C₆₀^{•−}. (c) EPR spectrum of the ET products derived from TTF-C4P and Li⁺@C₆₀. Adopted with permission from *J. Am. Chem. Soc.*, 2011, **133**, 15938, copyright 2011, American Chemical Society (ACS).

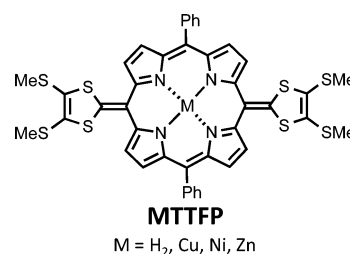


Fig. 6 Structure of quinoidal π -extended TTF porphyrins (MTTFP).

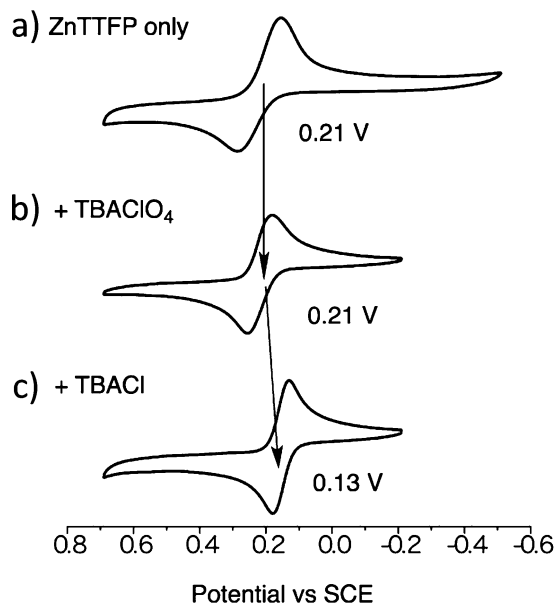


Fig. 7 CV of ZnTTFP in benzonitrile with (a) CV only in the presence of TBAPF₆ as a supporting electrolyte, (b) upon the addition of 10 equiv. of TBAClO₄ and (c) upon the addition of 10 equiv. of TBACl, leading to a shift in the oxidation wave. Reprinted with permission from *J. Am. Chem. Soc.*, 2013, **135**, 10852, copyright 2013, ACS.

by 0.15 V compared to the freebase analogue, H₂TTFP. ZnTTFP is oxidized at 0.21 V relative to SCE (Fig. 7a), a value near the first reduction potential of Li⁺@C₆₀ (0.13 V vs. SCE).

Further studies with ZnTTFP revealed that the zinc center is capable of forming a coordination bond with axial ligands. When the redox potential of ZnTTFP was reevaluated in the presence of chloride, a further anodic shift, to 0.13 V vs. SCE, was noted (Fig. 7c). This latter value matches well with the first reduction of Li⁺@C₆₀. We thus hypothesized that chloride anion coordination could induce thermodynamically favorable ET from ZnTTFP to Li⁺@C₆₀.

In accord with the above prediction, no evidence of ET was seen for a mixture of ZnTTFP and Li⁺@C₆₀ in benzonitrile in the absence of an axial ligand, as inferred from absorption spectroscopic analyses. The addition of a non-coordinating anion, such as PF₆[−] or BF₄[−], had no discernible effect on the system. However, the introduction of chloride (as TBACl) led to the appearance of bands associated with ZnTTFP^{•+} and Li⁺@C₆₀^{•−}, which was taken as evidence of ground state ET. The electron transfer equilibrium constant for this interaction was determined to be 0.53 based on a titration of Li⁺@C₆₀ into ZnTTFP in the presence of excess chloride (Fig. 8). A similar interaction was observed upon treatment of the system with the corresponding Br[−] salt.

Pyridine, on the other hand, did not induce ET upon binding to the zinc center. CV studies revealed that complexation of ZnTTFP with pyridine produced little to no effect on the redox potential of the system. On the other hand, we found that treating the chloride-bound, post-ET state Cl[−]·ZnTTFP^{•+}·Li⁺@C₆₀^{•−} with excess pyridine promoted back electron transfer and regeneration of ZnTTFP and Li⁺@C₆₀. Such a finding was

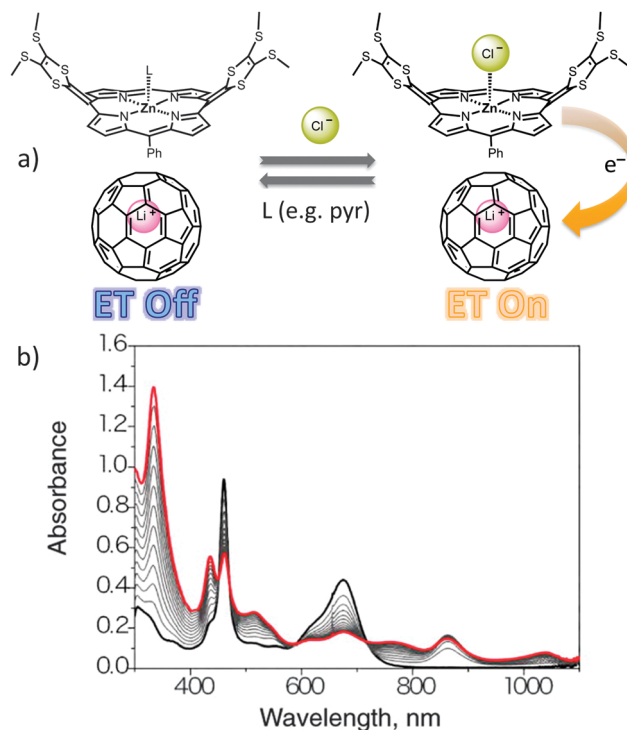


Fig. 8 (a) Schematic diagram of ZnTTFP serving as a ET switch, modulated by the addition of chloride and pyridine. (b) Absorption spectral changes of ZnTTFP in the presence of TBACl upon the successive addition of Li⁺@C₆₀ in benzonitrile. The black line is the original and the red is the final spectrum. Adapted with permission from *J. Am. Chem. Soc.*, 2013, **135**, 10852, copyright 2013, ACS.

ascribed to competitive displacement of the Cl[−] ligand from the metal center *via* the addition of pyridine and a commensurate restoration of energy levels that are unfavorable for ground state ET. This system thus complements those based on TTF-C4P and expands the lexicon of small molecules and ions whose presence or absence may be sensed as the result of favorable or unfavorable ET processes.

3.3 Intramolecular ET systems

In contrast to the examples in Section 3.2, wherein modification of the environmental surroundings (or external stimuli) promotes or inhibits intraensemble ET, intramolecular electron transfer (IET) within a covalently linked framework also represents a viable option in terms of ET-based sensing. For instance, in an elaborated molecular construct containing *multiple* appropriately tuned redox active sites, alteration of the molecular conformation, solvent system, or electronics of the electroactive components can induce ET from one portion of the molecule to another. In turn, this leads to changes in the electronic features of the molecule as a whole. Since, the resulting differences can typically be distinguished by a variety of standard methods (e.g., absorption spectroscopy, CV analyses, or conductivity measurements) the environmentally induced changes in the electronic features provide the readout function and the basis for molecular sensor development. Within the context of this potentially general paradigm, systems based on porphyrinoids are particularly

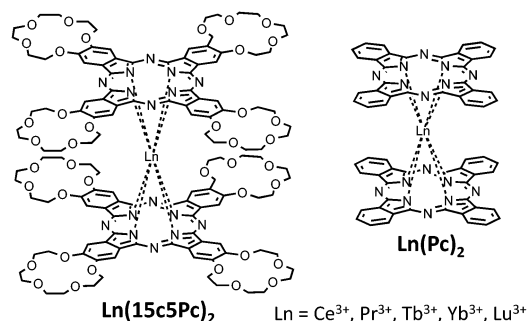


Fig. 9 Schematic representation of sandwich-type phthalocyanine complexes with lanthanides.

attractive. Porphyrinoid ligands are strong dyes with well-defined redox states, simplifying the detection of the IET event. Moreover, they typically serve as very effective ligands for redox active metal cations, which allows complexation-based sensing scenarios to be envisioned.

One example of IET involving a porphyrinoid system was reported recently by Selektor. It relies on a Pc-based sandwich-type complex (Fig. 9), namely cerium bis-[tetra(15-crown-5)-phthalocyanate] ($\text{Ce}(\text{15c5Pc})_2$).³¹ Pioneered by Kobayashi,³² phthalocyanines bearing crown-ether moieties on the periphery were found to stabilize a variety of supramolecular assemblies with novel optical properties.³³ Both donor-acceptor interactions between neighboring crown ether-bearing phthalocyanines (Pc) and supramolecular crown ether-cation associations are thought to stabilize these ensembles. Early on, these systems were studied with a view to their interesting photoinduced electron transfer features (*cf.* PET, Section 4.2).³⁴ Recently however, the ground state IET of these molecules was probed in the context of exploring the lanthanide cation complexation features of these elaborated Pcs.

Complexation of large metals, including lanthanide cations, by Pcs leads to 2 : 1 Pc to metal double-decker structures.³⁵ With regards to IET applications, cerium, the second largest “rare-earth” metal, is of particular interest. Unlike most of the other lanthanide cations (which are normally found in their +3 oxidation state) cerium has a readily accessible +4 oxidation state as a result of the stability of the $4f^0$ electron configuration. Depending on the substitution pattern of the tetrapyrrolic ligands bound to the cerium metal, overall neutral complexes but differing in the oxidation state of cerium and hence the charge on the ligand, have been reported.³⁶

Selektor and coworkers studied the physicochemical properties of Langmuir-type monolayer films of $\text{Ce}(\text{15c5Pc})_2$. The absorption spectrum of the $\text{Ce}(\text{15c5Pc})_2$ film (recorded by differential-reflection absorption spectrometry) was substantially different from that of the chloroform solution from which it was cast (Fig. 10). Specifically, the intensity of the Q-bands at 530 nm and 700 nm was seen to increase, while a concurrent decrease in the Q-band intensity at 650 nm was observed. Based on previous reports,³⁶ the authors considered the latter spectral features indicative of a Pc radical anion, due to the increased intensity of the band at 530 nm. However, it was unclear whether the Pc

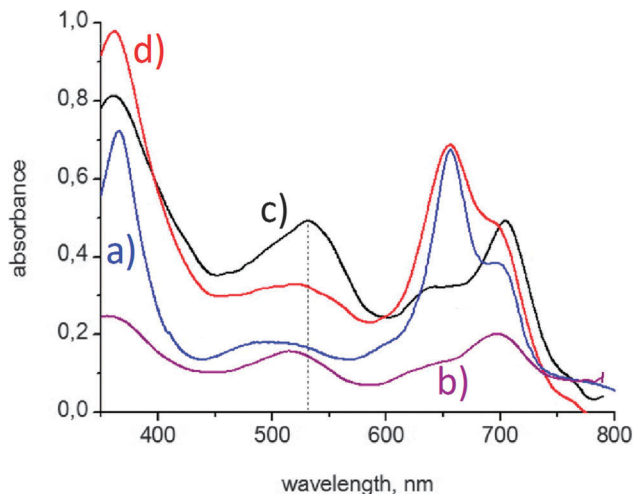


Fig. 10 Absorption spectra of $\text{Ce}(\text{15c5Pc})_2$ in (a) chloroform solution and monolayers (b) just after spreading at surface pressure, (c) at 20 mN m^{-1} and (d) at 35 mN m^{-1} . The intensities of b–d have been increased ($20\times$) for ease of comparison. Adapted with permission from *J. Phys. Chem. C*, 2014, **118**, 4250, copyright 2014, ACS.

core was oxidized by an external oxidant or as the result of internal electron transfer to the metal center (IET, *i.e.*, $\text{Ce}^{4+} \rightarrow \text{Ce}^{3+}$). To clarify which pathway led to the observed oxidation, monolayers of various other double-decker lanthanide complexes ($\text{Ln}(\text{15c5Pc})_2$ where $\text{Ln} = \text{Pr}^{3+}, \text{Tb}^{3+}, \text{Yb}^{3+}$, and Lu^{3+}) were prepared and investigated. In contrast to what was seen with cerium, in the case of the control lanthanide(III) films, the absorption spectra of the monolayers closely matched their respective solution state spectra. Additionally, all the control films were characterized by Q-type bands with absorption maxima near 500 nm, which was taken as evidence for an unpaired electron within the Pc ring. In contrast, the unsubstituted cerium sandwich complex, CePc_2 , which is known to contain a tetravalent (Ce^{4+}) cation, displays no appreciable absorption intensity in the 500 nm spectral region.^{34,36} On the basis of this comparison, as well as other considerations, the authors concluded that in solution the Ce^{4+} oxidation state dominates for the $\text{Ce}(\text{15c5Pc})_2$ complex, but upon the formation of monolayers, IET leads to the Ce^{3+} oxidation state predominating.

The driving force for IET occurring in $\text{Ce}(\text{15c5Pc})_2$ upon the transfer of the molecule from an organic solvent environment to monolayer films is multifaceted. At atmospheric pressure, the Pc rings of $\text{Ce}(\text{15c5Pc})_2$ monolayers were found to sit parallel to the air–water interface in a “face-on” orientation. The effects of this arrangement are twofold. First, it modifies the local solvent environment of one Pc ring, increasing the hydration of the Pc nearest the water interface. Second, the interactions of one Pc face of $\text{Ce}(\text{15c5Pc})_2$ with the polar subphase breaks the electronic symmetry of the complex, increasing the mobility of the π -electrons and lowering the barrier to IET. It is hypothesized that to compensate for the asymmetric hydration, an electron is transferred from a Pc ring to the cerium metal *via* IET. To the extent this is true $\text{Ce}(\text{15c5Pc})_2$ serves as a rudimentary environmental IET-based sensor.

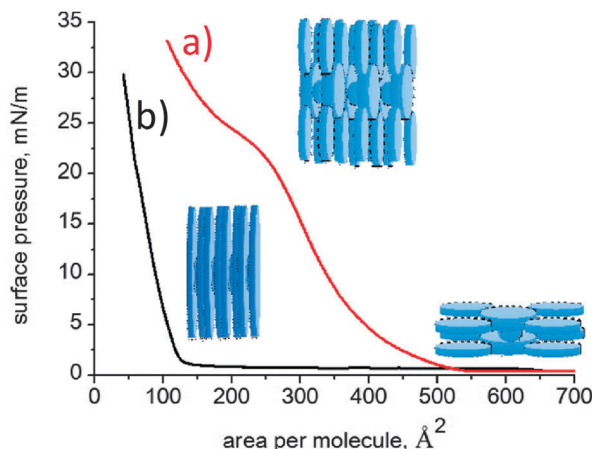


Fig. 11 Compression isotherms of (a) $\text{Ce}(\text{15c5Pc})_2$ and (b) CePc_2 . The insets show a proposed model for the orientation of the constituent macrocycles. Adapted with permission from *J. Phys. Chem. C*, 2014, **118**, 4250, copyright 2014, ACS.

Interestingly, compression of $\text{Ce}(\text{15c5Pc})_2$ monolayers results in the reformation of the Ce^{4+} oxidation state. Above 27 mN m^{-1} pressure, the absorption spectra of $\text{Ce}(\text{15c5Pc})_2$ monolayers reverts to a pattern similar to that of the solution-state spectra (Fig. 11). Compression isotherms are consistent with a normal decrease in the mean molecular area upon pressurization up until 20 mN m^{-1} . After this, a plateau region is attained (from ca. 20 – 27 mN m^{-1}), wherein normal increases in pressure lead to a larger than expected compression of the mean molecular area. Such findings are attributed to the translation of individual $\text{Ce}(\text{15c5Pc})_2$ molecules from a face-on arrangement to one wherein the disc-like molecules are located perpendicular to the air–water interface. Above 27 mN m^{-1} normal compression behavior resumes, as would be expected for scenario wherein full conversion of the monolayers to a perpendicular orientation occurs. The perpendicular arrangement of $\text{Ce}(\text{15c5Pc})_2$ obviates the increased stabilization of the Ce^{3+} state expected in the monolayer as the result, presumably of increased asymmetrical hydration and polarization, resulting in reversion to the Ce^{4+} oxidation state seen in organic media. At high pressures, the conversion of Ce^{3+} to Ce^{4+} is considered favorable due to the smaller ionic radius associated with the higher oxidation state. Since the changes can be followed by absorption spectroscopy, the IET effects allow the $\text{Ce}(\text{15c5Pc})_2$ films to serve as molecular-based pressure sensors.

4. Photoinduced ET (PET) systems

4.1 Biological systems

The complexity, functionality and efficiency of photosynthetic systems can be considered as the culmination of billions of years of evolution involving *inter alia* biological switches. In this context, photosystem II (PSII) deserves special mention since it is composed of a protein–pigment complex of 20 subunits and approximately 100 cofactors.³⁷ The main harvesters of light in PSII are oligopyrrolic chlorophylls assembled in antennae-type

structures. Further, the oxygen-evolving complex of PSII is known to be activated by the presence of Cl^- and Ca^{2+} ions.³⁸ Thus, in an oversimplified view, PSII can be considered as an oligopyrrolic-containing complex of photo- and pH-dependent switches that utilizes energy collected *via* photoexcitation to feed a cascade of proton-coupled electron transfer processes that eventually result in the production of oxygen.

4.2 Synthetic oligopyrrolic systems

Driven by a desire to replace environmentally hazardous carbon-based fuels for worldwide energy demands, a large body of work has been devoted to fabricating synthetic mimics of photosynthesis. Oligopyrrolic macrocycles have played a key role in this pursuit, as a result of their large molar absorptivities and, in turn, the ease with which their higher electronic states may be populated by solar radiation.³⁹ To date, many oligopyrrolic donor–acceptor systems have been reported in which ET does not occur spontaneously from the ground state but instead requires the formation of an excited state of one or both of the constituents to drive the ET process forward.

Although representing an application orthogonal to that which inspired their original synthesis, many of these systems have the potential to be “rebranded” as PET-based molecular switches or sensors. In this section we will highlight several recent porphyrinogen-based supramolecular systems that demonstrate switchable photoinduced electron transfer upon tuning the electronic character of one of the partners that makes up the self-associated complex. We will focus on examples from our groups, with a particular emphasis given to those systems that have not been previously reviewed. Many others, including D’Souza and Fukuzumi, have made integral contributions to this area and the interested reader is encouraged to explore the literature devoted to this topic.^{8a,10,40}

4.2.1 Androgynous (donor and acceptor) systems. Recently, we described a system in which cyclo[8]pyrrole (C8), in its diprotonated form, revealed *androgynous* electronic characteristics (Fig. 12).⁴¹ As a result of its rather small HOMO–LUMO gap (0.60 eV), C8 can act as both an electronic donor and acceptor

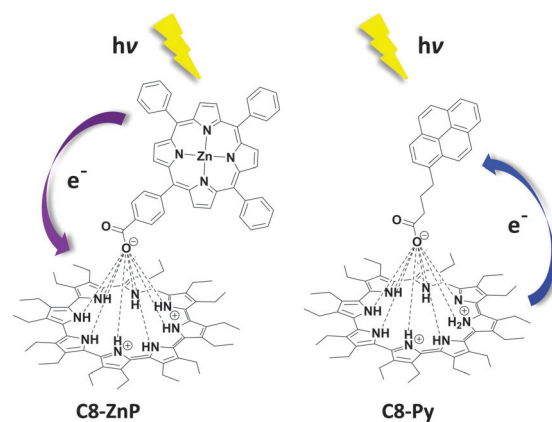


Fig. 12 Androgynous PET based on carboxylate binding to cyclo[8]pyrrole (C8). The direction of PET is from ZnP to C8 in C8–ZnP hybrid, and reversed in C8–Py association complex.

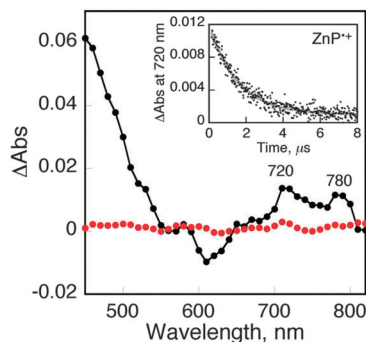


Fig. 13 Transient absorption spectra of C8-ZnP ([C8] = 5.0×10^{-5} M, [ZnP] = 5.0×10^{-5} M) recorded in deaerated MeCN at r.t. The spectra were recorded 0.5 μ s (black line) and 8.0 μ s (red line) after nanosecond laser photoexcitation (440 nm, 10 mJ per pulse). Inset: decay time profile of the absorbance feature at 720 nm ascribed to ZnP $^{\bullet+}$ present in the CS ensemble. Adapted with permission from *J. Phys. Chem. C*, 2014, **118**, 18436, copyright 2014, ACS.

depending on the redox partner to which it is exposed. This makes it a prototypical ET-based molecular sensor system. For example, when combined with a zinc porphyrin carboxylate (ZnP), C8 forms a 1 : 1 supramolecular complex (C8-ZnP) stabilized *via* a combination of hydrogen bonding and electrostatic interactions. When this complex is subject to nanosecond laser photoexcitation at 430 nm in acetonitrile, electron transfer occurs from the triplet excited state of the porphyrin ($^3\text{ZnP}^*$) to C8. This results in formation of the corresponding charge separated (CS) state, C8 $^{\bullet-}$ -ZnP $^{\bullet+}$. The CS state was characterized by transient absorption spectroscopy (TAS), an analysis that revealed transient spectral features at 720/780 nm and 1000 nm corresponding to ZnP $^{\bullet+}$ and C8 $^{\bullet-}$, respectively (Fig. 13). Under these conditions, C8 thus acts as an electron acceptor.

In contrast, C8 acts as an electron acceptor when ZnP is replaced by a pyrenyl carboxylate (Py) (Fig. 12). In this case, irradiation of the C8-Py complex (formed by simple mixing in organic media) at 440 nm produces spectral signals consistent with the transfer of an electron from C8 to the singlet excited state of the pyrene partner (1Py *). This results in formation of a C8 $^{\bullet+}$ -Py $^{\bullet-}$ complex,⁴² as evidenced by the presence of TAS features corresponding to C8 $^{\bullet+}$ (peaks at 450, 740, and 820 nm) and, Py $^{\bullet-}$ (480 nm). PET occurs in the C8 \rightarrow Py direction despite the calculated energy of the C8 $^{\bullet+}$ -Py $^{\bullet-}$ complex (2.58 eV) being higher than that of putative C8 $^{\bullet-}$ -Py $^{\bullet+}$ state (1.31 eV).

Marcus theory provides a rational for the fact that the higher energy C8 $^{\bullet+}$ -Py $^{\bullet-}$ complex is formed in preference. Specifically, it predicts that formation of the lower energy state (C8 $^{\bullet-}$ -Py $^{\bullet+}$) is well within the Marcus inverted region, a finding that is consistent with the drastically diminished rate with which this hypothetical complex is formed. Independent of the theoretical underpinnings, the fact that the direction of ET can be controlled by changing the redox partner leads us to suggest that C8 can be considered a simple supramolecular PET switch that responds to (at least) two specific analytes, namely ZnP and Py.

4.2.2 Phthalocyanine-graphene complexes. Switchable PET effects have also been reported among supramolecular systems

incorporating phthalocyanines (Pc) with carbon-rich nanostructures (CNS, *e.g.*, graphene, carbon nanotubes, and fullerenes). In contrast to the previously described examples utilizing C8 (in which the oligopyrrole acts as the androgynous PET switch), in Pc-CNS complexes, the electronic nature of the Pcs have been modulated to effect a switching of the direction of PET toward the CNS.

Graphene is characterized by a high density of states above and below the Fermi level and, as such, may be considered as a zero band gap semiconductor.⁴³ Therefore, graphene has been utilized as both an electron donor and an electron acceptor. This makes it a prime candidate for incorporation into switches based on PET. Several *covalently* linked nanohybrids of graphene with electron-rich⁴⁴ or electron-deficient⁴⁵ Pcs in which the direction of PET was dictated by the electronic nature of the appended Pc have been previously described. In this Feature, however, we will concentrate on summarizing non-covalent systems involving graphene and Pcs.

The electronic characteristics of graphene flakes were found to be detectably altered by supramolecular association with a ZnPc poly(*p*-phenylenevinylene) polymer bearing cyano groups (ZnPc-PPV-CN) (Fig. 14).⁴⁶ ZnPc-PPV-CN, containing a string of pendant ZnPc units along its polymeric backbone, was found to associate strongly with nanographene (NG). ZnPc-PPV-CN assists in the exfoliation of graphite and stabilizes the newly formed flakes that were found to contain 2–3 layers of graphene. Surprisingly, evidence of strong electronic coupling between the individual components was seen in the ZnPc-PPV-CN-NG aggregates even in the ground-state. Specifically, the absorption of the Q-band of ZnPc was shifted to 707 nm, in comparison with 675 nm for free ZnPc-PPV-CN in THF (Fig. 15). Additionally, upon interaction with NG, the fluorescence of ZnPc was quenched. This was taken as evidence of electron transfer from ZnPc to graphene in the excited state. Additional evidence was obtained from TAS of the ZnPc-PPV-CN-NG hybrid employing femtosecond flash photolysis in THF (700 nm). In these studies, the appearance of a peak at 840 nm was noted. Such a feature is characteristic of the one-electron oxidized form of ZnPc. Hence, in the current system photoexcitation of the ZnPc moieties leads to efficient PET from ZnPc to graphene, with the latter species acting as an electron acceptor.

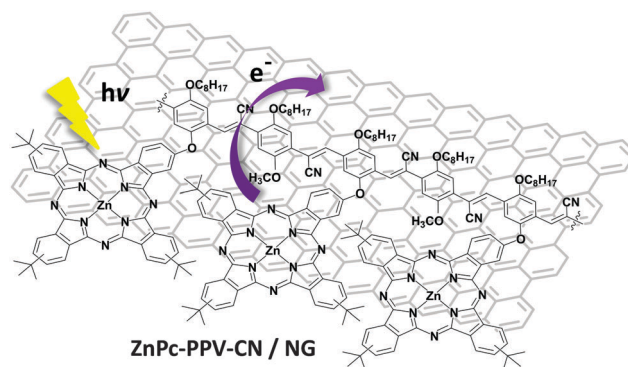


Fig. 14 Proposed structure of an exfoliated graphene-ZnPc-PPV-CN nanohybrid (termed ZnPc-PPV-CN/NG).

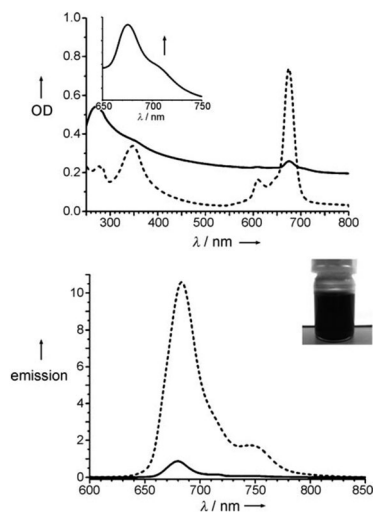


Fig. 15 (top) Absorption spectra of ZnPc-PPV-CN (dashed line) and ZnPc-PPV-CN/NG (solid line) recorded in THF; the inset shows the 650 to 750 nm range. (down) Emission spectra of ZnPc-PPV-CN (dashed line) and ZnPc-PPV-CN/NG (solid line) recorded in THF. Reproduced from ref. 46 by permission of John Wiley & Sons Ltd.

Pc-NG systems have also helped shed light on the less-well explored electron donating features of graphene. For instance, by exploiting π - π interactions, a pyrene-functionalized (alkylsulfonyl) zinc(II) phthalocyanine (ZnPc-Py) could be bound to highly exfoliated graphite (Fig. 16).⁴⁷ The reduction potential of ZnPc-Py is relatively low, as would be expected given the electron withdrawing sulfonyl ester groups. As a result, this particular porphyrinoid species is electron deficient. It acts an electron acceptor when mixed with NG sheets. Evidence for strong electronic interactions was seen in both the ground and excited states. Upon photoexcitation of the ZnPc-Py-NG complex at 387 nm, a CS state was generated (*i.e.* ZnPc-Py^{•-}-NG^{•+}) that undergoes slow charge recombination. TAS maxima at 485, 582, and 760 nm and minima at 460 and 640 nm were observed that were considered as “fingerprints” of the one-electron reduced radical anion ZnPc-Py^{•-} (Fig. 16), supporting

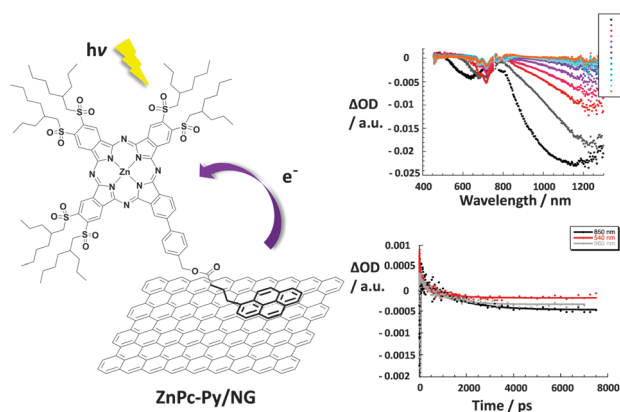


Fig. 16 (left) Proposed structure of an (alkylsulfonyl) ZnPc-pyrene-graphene nanohybrid (ZnPc-Py/NG). (right) Differential absorption obtained upon femto-second pump probe excitation (387 nm) of ZnPc-Py/NG in DMF. Adapted from ref. 47 with permission from The Royal Society of Chemistry.

the formation of the transient CS state. Other new features evolved during the transient decay, including broad maxima at 950 and 1070 nm that were interpreted in terms of the formation of new holes in the valence band of graphene. When considered in conjunction with the previous example involving ZnPc-PPV-CN, the studies with (alkylsulfonyl) ZnPc-Py provide support for the notion that sheets of NG may serve as an ambidirectional supramolecular PET partner when paired with appropriately tuned Pc compounds. As such, it becomes appealing to envision new kinds of ET switches based on NG and appropriately designed Pc constructs.

4.2.3 Phthalocyanine-carbon nanotube complexes. Carbon nanotubes (CNT) are also attractive building blocks for the construction of potential ET-based sensors. As true for NG, CNTs display semiconducting character. They are thus expected to act as both electron donors and electron acceptors depending on the electronic partners with which they are paired.⁴⁸ Recent reports on charge transfer reactions involving CNTs in heterojunctions, as well as their use as electron donors in photoelectrochemical cells⁴⁹ and organic field-effect transistors,⁵⁰ attest to the considerable interest and active research in the area of CNT-based devices.

Our experience with ZnPc-PPV-CN/NG conjugates inspired us to try dispersing single-walled CNTs (SWNT) *via* the use of various Pc-poly(*p*-phenylenevinylene)s (Pc-PPVs). Upon mixing of SWNTs with ZnPc-PPV-CN (Fig. 17) stable and finely dispersed suspensions were obtained. These suspensions were characterized by means of absorption and Raman spectroscopy, as well as atomic force microscopy. In contrast, oligomers ZnPc-PPV lacking a cyano group failed to suspend the CNTs,⁵¹ as evidenced by the absence of spectroscopically viable SWNT suspensions. The electronic nature of the Pc-PPV oligomers was used to rationalize these experimental findings. In the case of oligomer ZnPc-PPV-CN, the presence of electron-withdrawing cyano substituents on PPV backbone imparts n-type character to the macromolecule, thus favoring strong π - π interactions with p-type SWNTs. In contrast, the PPV oligomers missing cyano functionalities along their backbone revealed p-type character and thus displayed a low affinity for the p-type SWNTs. TAS measurements carried out on the ZnPc-PPV-CN-SWNT supramolecular hybrid revealed the formation of a metastable charge-separated photoproduct (Pc^{•+}-SWNT^{•-}), presumably reflecting the presence of stabilizing n-type-p-type interactions between the respective partners.

Modification of the original p-type Pc-PPV systems to impart improved structural flexibility led remarkably to the formation

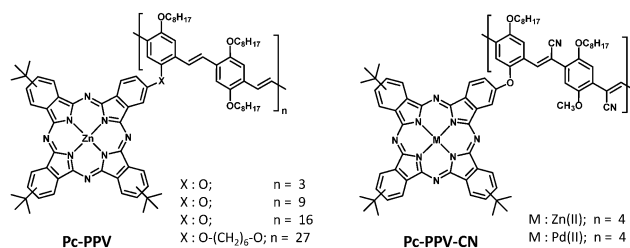


Fig. 17 Structures of Pc-PPV oligomers used for the construction of nanohybrids with SWNTs.

of stable suspensions when exposed to p-type SWNTs.⁵² Time-resolved TAS measurements of confirmed PET from the photo-excited ZnPc to the SWNT resulting in a CS state that was stable for 100 ps.

Recent studies have led to improvements in our ability to immobilize Pc-PPV-CN oligomers onto SWNTs. Specifically, we have replaced pristine SWNTs with C₆₀@SWNT peapods. The latter species form stronger complexes with Pc-PPV-CN oligomers most likely as the result of an intrinsic charge transfer from the SWCNTs to the encapsulated C₆₀, which serves to increase its p-type character.⁵³ In analogy to what was seen with SWCNTs, PET and injection of an electron from the Pc motif into the conduction band of SWCNTs was observed upon photoexcitation of the self-assembled Pc-PPV-CN-C₆₀@SWNT ensemble.

Pyrene-substituted phthalocyanines have also been explored for the construction of supramolecular hybrids with SWNTs, with the direction of photoinduced electron transfer likewise being studied.⁵⁴ As expected, Pc-Py (a and b, Fig. 18) were found to adhere to periphery of the SWNTs by means of π - π interactions. In fact, mixtures of these components result in the formation of stable suspensions. Upon photoexcitation of these suspensions at 387 nm, PET from the singlet excited state of either Pc-Py to the SWNT partners was observed. This ET event was evidenced by the observation of transient features characteristic of the Pc radical cation (*i.e.*, maxima at 520 and 840 nm) and the SWNT radical anion (*e.g.*, a negative imprint associated with the van Hove singularities at 1000–1600 nm (Fig. 18)).

Pyrenyl-bound azuleno-cyanine (azPc-Py) (Fig. 19) was synthesized to expand upon the results obtained with the Pc-Py-SWNT ensemble suspensions.⁵⁵ As expected, immobilization of azuleno-cyanine derivatives onto SWNT surfaces yielded supramolecular associates that were strongly electronically coupled in the ground state, allowing rapid charge separation in the excited state. Charge recombination of 137 ps was observed for azPc-Py-SWNT system, that is faster than that of Pc-Py-SWNT (beyond 3 ns). This

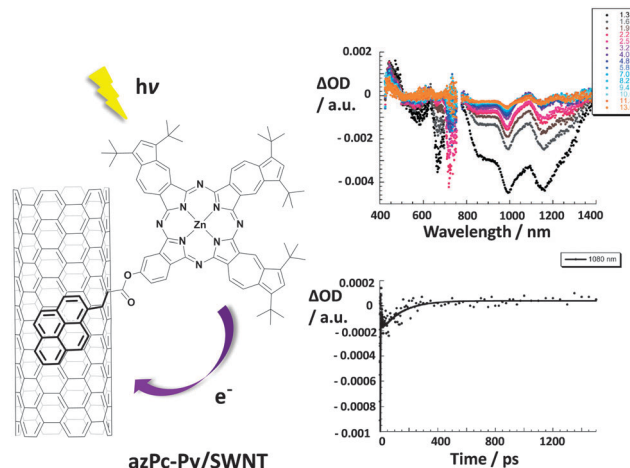


Fig. 19 (left) Structure of azuleno-cyanine-pyrene-SWNT nanohybrid (only one of the various possible isomers is shown). (right) Differential absorption spectra obtained upon femtosecond pump-probe experiments (387 nm) of azPc-Py-SWNT in 25% THF–75% DMF with different time delays between 1.3 and 13.0 ps at room temperature and time absorption profile at 1080 nm. Adapted from ref. 55 with permission from The Royal Society of Chemistry.

difference leads us to suggest that such systems could provide the basis for differentiating ostensibly similar PET partners thus providing a new, electron transfer-based approach to sensing.

Although many examples wherein Pcs serve as PET donors to carbon nanotubes are known, to our knowledge systems that exploit electron-deficient Pcs as electron acceptors have yet to be reported. Studies along these lines are ongoing in our laboratories. If successful, these efforts may allow CNTs to emerge as PET-based sensors for particular classes of Pcs (*e.g.*, electron rich vs. electron deficient).

Subphthalocyanines (SubPc) are a relatively underexplored class of molecules that may prove particularly useful in the context of developing new PET-based switching systems.⁵⁶ In addition to having received attention for their unique photophysical properties, SubPc have attracted interest as easy-to-manipulate components for molecular self-assembly. For instance, SubPcs have been recently used to construct supramolecular jelly fish-like ensembles⁵⁷ and for SubPc-based metallosupramolecular encapsulation.⁵⁸ In both cases, photoexcitation of the SubPc supramolecular hybrids is followed by singlet excited-state energy transfer to a complexed fullerene receptor. Additionally, covalent constructs containing SubPcs have been demonstrated to undergo efficient photo-induced electron transfer reactions, with the SubPcs acting as either electron donors or acceptors.⁵⁹ Because of this latter duality, we predict that SubPcs will emerge as important constituents in PET-based electron switches, molecular sensors, and synthetic logic gates. However, to date this promise has yet to be realized.

5. Conclusions

While much remains to be done, we believe that the foundations have been laid for electron transfer processes (both thermodynamic and photoinduced) to emerge a new tool in

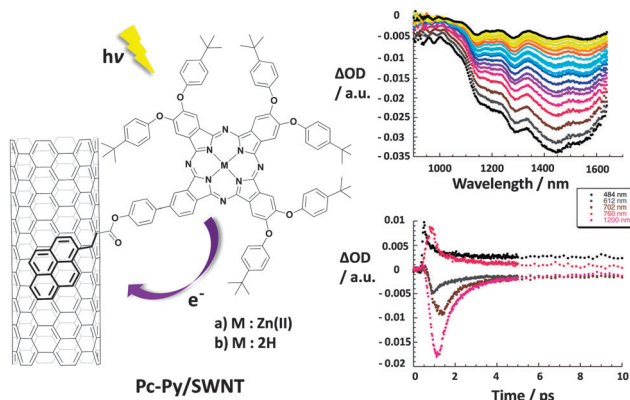


Fig. 18 (left) Structure of a hexakis(4-tert-butylphenoxy)-ZnPc-Pyrene-SWNT nanohybrid. (right) Differential absorption spectra (extended near-infrared) obtained upon femtosecond flash photolysis (387 nm) of ZnPc-Py-SWNT in 25% THF–75% DMF recorded at several time delays between 0 and 10 ps at room temperature and time-absorption profiles of spectra shown above at 484, 612, 702, 760, and 1200 nm, monitoring the charge separation. Adapted with permission from *J. Am. Chem. Soc.*, 2010, **132**, 16202, copyright 2010, ACS.

the proverbial toolbox associated with molecular sensing and switching. Because recognition, detection, and logic functions are not typically foremost considerations in the design of, e.g., artificial photosynthetic systems, ET events have hitherto mostly been overlooked in the context of molecular sensor and switch development. As a consequence, there is room for considerable growth. Key challenges going forward involve generalizing the paradigm and developing systems with increased specificity, greater robustness, and an ability to respond to an expanded range of analytes. It is the hope of the authors that this Feature will inspire additional efforts to exploit ET phenomena for the purpose of molecular sensing and logic design. The orthogonal nature of the ET-based approach, relative to more established modalities, makes this vision particularly appealing.

Acknowledgements

The work in Austin was supported by the U.S. National Science Foundation (grant CHE-1402004 to J.L.S.) and the Robert A. Welch Foundation (Grant F-1018 to J.L.S.). Financial support from the Spanish MICINN (CTQ2011-24187/BQU) and the Comunidad de Madrid (S2013/MIT-2841 FOTOCARBON) is acknowledged.

Notes and references

- For recent examples see and references therein: (a) X. Zhang, Y. Yin and J. Yoon, *Chem. Rev.*, 2014, **114**, 4918; (b) H. N. Kim, X. Wen, J. S. Kim and J. Yoon, *Chem. Soc. Rev.*, 2012, **41**, 3210; (c) Y. Zhou and J. Yoon, *Chem. Soc. Rev.*, 2012, **41**, 52.
- For recent examples see and references therein: (a) K. P. Carter, A. M. Young and A. E. Palmer, *Chem. Rev.*, 2014, **114**, 4564; (b) N. Dai and E. T. Kool, *Chem. Soc. Rev.*, 2011, **40**, 5755.
- For examples, see: (a) K. Abe, D. Ogasawara, W. Yoshida, K. Sode and K. Ikebukuro, *Faraday Discuss.*, 2011, **149**, 93; (b) J. S. Kim and D. T. Quang, *Chem. Rev.*, 2007, **107**, 3780.
- For examples, see: (a) J. L. Segura and N. Martin, *Angew. Chem., Int. Ed.*, 2001, **40**, 1372; (b) S. J. Toal and W. C. Trögl, *J. Mater. Chem.*, 2006, **16**, 2871; (c) P. A. Gale, P. Anzenbacher and J. L. Sessler, *Coord. Chem. Rev.*, 2001, **222**, 57.
- U. Lange, N. V. Roznyatovskaya and V. M. Mirsky, *Anal. Chim. Acta*, 2008, **614**, 1.
- F. Deiss, N. Sojic, D. J. White and P. R. Stoddart, *Anal. Bioanal. Chem.*, 2010, **396**, 53.
- Y. L. Zhao, L. Hu, J. F. Stoddart and G. Grüner, *Adv. Mater.*, 2008, **20**, 1910.
- (a) S. Fukuzumi, K. Ohkubo, F. D'Souza and J. L. Sessler, *Chem. Commun.*, 2012, **48**, 9801; (b) J. L. Sessler, B. Wang, S. L. Springs and C. T. Brown, *Compr. Supramol. Chem.*, 1996, **4**, 311.
- (a) M. R. Wasielewski, *Chem. Rev.*, 1992, **92**, 435; (b) D. Gust, T. A. Moore and A. L. Moore, *Acc. Chem. Res.*, 1999, **28**, 263; (c) M. D. Ward, *Chem. Soc. Rev.*, 1997, **26**, 365; (d) F. M. Raymo and M. Tomasulo, *Chem. Soc. Rev.*, 2005, **34**, 327; (e) M.-J. Blanco, M. Consuelo Jimenez, J.-C. Chambron, V. Heitz, M. Linke and J.-P. Sauvage, *Chem. Soc. Rev.*, 1999, **28**, 293; (f) *Electron Transfer in Chemistry*, ed. V. Balzani, Wiley-VCH, Weinheim, 2001.
- (a) F. D'Souza and O. Ito, *Chem. Commun.*, 2009, 4913; (b) F. D'Souza and O. Ito, *Coord. Chem. Rev.*, 2005, **249**, 1410; (c) M. E. El-Khouly, O. Ito, P. M. Smith and F. D'Souza, *J. Photochem. Photobiol., C*, 2004, **5**, 79; (d) F. D'Souza and O. Ito, *Coord. Chem. Rev.*, 2005, **249**, 1410; (e) R. Chitta and F. D'Souza, *J. Mater. Chem.*, 2008, **18**, 1440.
- (a) F. D'Souza, E. Maligaspe, K. Ohkubo, M. E. Zandler, N. K. Subbaiyan and S. Fukuzumi, *J. Am. Chem. Soc.*, 2009, **131**, 8787; (b) T. Kojima, T. Honda, K. Ohkubo, M. Shiro, T. Kusukawa, T. Fukuda, N. Kobayashi and S. Fukuzumi, *Angew. Chem., Int. Ed.*, 2008, **47**, 6712; (c) M. Tanaka, K. Ohkubo, C. P. Gros, R. Guillard and S. Fukuzumi, *J. Am. Chem. Soc.*, 2006, **128**, 14625; (d) A. Takai, C. P. Gros, J.-M. Barbe, R. Guillard and S. Fukuzumi, *Chem. – Eur. J.*, 2009, **15**, 3110; (e) A. Takai, M. Chkounda, A. Eggenspieler, C. P. Gros, M. Lachkar, J.-M. Barbe and S. Fukuzumi, *J. Am. Chem. Soc.*, 2010, **132**, 4477.
- The Porphyrin Handbook*, ed. K. M. Kadish, K. M. Smith and R. Guillard, Academic Press, San Diego, CA, 2000, vol. 1–20.
- R. A. Marcus, *Angew. Chem., Int. Ed. Engl.*, 1993, **32**, 1111.
- (a) J. Franck, *Trans. Faraday Soc.*, 1926, **21**, 536; (b) E. Condon, *Phys. Rev.*, 1926, **27**, 640.
- R. A. Marcus, *J. Chem. Phys.*, 1956, **24**, 966.
- R. A. Marcus, *Discuss. Faraday Soc.*, 1960, **29**, 21.
- J. R. Miller, L. T. Calcaterra and G. L. Closs, *J. Am. Chem. Soc.*, 1984, **106**, 3047.
- H. Lodish, A. Berk, C. A. Kaiser, M. Krieger, A. Bretscher, H. Ploegy, A. Amon and M. P. Scott, *Molecular Cell Biology*, W. H. Freeman Publishers, San Francisco, 7th edn, 2012.
- H. B. Gray, in *Electron Transfer in Bioinorganic Chemistry*, ed. I. Bertini, H. B. Gray, S. J. Lippard and J. S. Valentine, University Science Books, Mill Valley, CA, 1994, pp. 315–363.
- (a) G. Battistuzzi, M. Borsari, D. Dallari, I. Lancellotti and M. Sola, *Eur. J. Biochem.*, 1996, **241**, 208; (b) X. Zhao, M. J. Nilges and Y. Lu, *Biochemistry*, 2005, **44**, 6559.
- K. A. Nielsen, W.-S. Cho, J. O. Jeppesen, V. M. Lynch, J. Becher and J. L. Sessler, *J. Am. Chem. Soc.*, 2004, **126**, 16296.
- A. G. Tennyson, R. J. Ono, T. W. Hudnall, D. M. Khramov, J. A. Er, J. W. Kamplain, V. M. Lynch, J. L. Sessler and C. W. Bielawski, *Chem. – Eur. J.*, 2010, **16**, 304.
- J. S. Park, E. Karnas, K. Ohkubo, P. Chen, K. M. Kadish, S. Fukuzumi, C. W. Bielawski, T. W. Hudnall, V. M. Lynch and J. L. Sessler, *Science*, 2010, **329**, 1324.
- (a) P. A. Gale, J. L. Sessler and V. Kral, *Chem. Commun.*, 1998, **1**; (b) J. L. Sessler and P. A. Gale, in *The Porphyrin Handbook*, ed. K. M. Kadish, K. M. Smith and R. Guillard, Academic Press, San Diego, CA, 2000, vol. 6, pp. 257–278.
- (a) J. L. Sessler, D. E. Gross, W.-S. Cho, V. M. Lynch, F. P. Schmidtchen, G. W. Bates, M. E. Light and P. A. Gale, *J. Am. Chem. Soc.*, 2006, **128**, 12281; (b) S. K. Kim and J. L. Sessler, *Acc. Chem. Res.*, 2014, **47**, 2525; (c) H. Miyaji, H.-K. Kim, E.-K. Sim, C.-K. Lee, W.-S. Cho, J. L. Sessler and C.-H. Lee, *J. Am. Chem. Soc.*, 2005, **127**, 12510; (d) S. K. Kim, J. L. Sessler, D. E. Gross, C.-H. Lee, J. S. Kim, V. M. Lynch, L. H. Delmau and B. P. Hay, *J. Am. Chem. Soc.*, 2010, **132**, 5827; (e) D. E. Gross, F. P. Schmidtchen, W. Antonius, P. A. Gale, V. M. Lynch and J. L. Sessler, *Chem. – Eur. J.*, 2008, **14**, 7822; (f) C. Caltagirone, N. L. Bill, D. E. Gross, M. E. Light, J. L. Sessler and P. A. Gale, *Org. Biomol. Chem.*, 2010, **8**, 96.
- (a) K. A. Nielsen, W.-S. Cho, J. Lyskawa, E. Levillain, V. M. Lynch, J. L. Sessler and J. O. Jeppesen, *J. Am. Chem. Soc.*, 2006, **128**, 2444; (b) K. A. Nielsen, W.-S. Cho, G. Sarova, B. M. Petersen, A. D. Bond, J. Becher, F. Jensen, D. M. Guldi, J. L. Sessler and J. O. Jeppesen, *Angew. Chem., Int. Ed.*, 2006, **45**, 6848.
- S. Fukuzumi, K. Ohkubo, Y. Kawashima, D. S. Kim, J. S. Park, A. Jana, V. Lynch, D. Kim and J. L. Sessler, *J. Am. Chem. Soc.*, 2011, **133**, 15938.
- (a) K. Ohkubo, Y. Kawashima and S. Fukuzumi, *Chem. Commun.*, 2012, **48**, 4314; (b) K. Ohkubo, Y. Kawashima and S. Fukuzumi, *Chem. Commun.*, 2012, **48**, 4314.
- (a) N. L. Bill, M. Ishida, S. Bähring, J. M. Lim, S. Lee, C. M. Davis, V. M. Lynch, K. A. Nielsen, J. O. Jeppesen, K. Ohkubo, S. Fukuzumi, D. Kim and J. L. Sessler, *J. Am. Chem. Soc.*, 2013, **135**, 10852; (b) N. L. Bill, M. Ishida, Y. Kawashima, K. Ohkubo, Y. M. Sung, V. M. Lynch, J. M. Lim, D. Kim, J. L. Sessler and S. Fukuzumi, *Chem. Sci.*, 2014, **5**, 3888.
- See the following, and references therein: (a) F. G. Brunetti, J. L. Lopez, C. Atienza and N. Martin, *J. Mater. Chem.*, 2012, **22**, 4188; (b) *TTF Chemistry: Fundamentals and Applications of Tetra-thiafulvalene*, ed. J. Yamada and T. Sugimoto, Springer, Berlin, 2004.
- S. L. Selektor, A. V. Shokurov, V. V. Arslanov, Y. G. Gorbunova, K. P. Birin, O. A. Raitman, F. Morote, T. Cohen-Bouhacina, C. Grauby-Heywang and A. Y. Tsivadze, *J. Phys. Chem. C*, 2014, **118**, 4250.
- (a) N. Kobayashi and A. B. P. Lever, *J. Am. Chem. Soc.*, 1986, **109**, 7433; (b) N. Kobayashi and Y. Nishiyama, *J. Chem. Soc., Chem. Commun.*, 1987, 1462.

- 33 Y. Gorbunova, A. Martynov and A. Tsivadze, in *Handbook of Porphyrin Science*, ed. K. M. Kadish, K. M. Smith and R. Guilard, World Scientific Publishing, Singapore, 2012, pp. 271–388, and references therein.
- 34 F. D'Souza, E. Maligaspe, A. S. D. Sandanayaka, K. Navaneetha, P. A. Karr, T. Hasobe and O. Ito, *J. Phys. Chem. A*, 2010, **114**, 10951.
- 35 D. K. P. Ng and J. Jiang, *Chem. Soc. Rev.*, 1997, **26**, 433.
- 36 (a) Y. Bian, J. Jiang, Y. Tao, M. T. M. Choi, R. Li, A. C. H. Ng, P. Zhu, N. Pan, X. Sun, D. P. Arnold, Z.-Y. Zhou, H.-W. Li, T. C. W. Mak and D. K. P. Ng, *J. Am. Chem. Soc.*, 2003, **125**, 12257; (b) J. Jiang, W. Liu, K.-W. Poon, D. Du, D. P. Arnold and D. K. P. Ng, *Eur. J. Inorg. Chem.*, 2000, 205; (c) K. P. Birin, Y. G. Gorbunova and A. Y. Tsivadze, *J. Porphyrins Phthalocyanines*, 2008, **12**, 1154.
- 37 Govindjee, J. F. Kern, J. Messinger and J. Whitmarsh, *Photosystem II, in eLS*, John Wiley & Sons Ltd., Chichester, 2nd edn, 2010.
- 38 (a) C. F. Yocum, *Coord. Chem. Rev.*, 2007, **252**, 296; (b) B. Loll, J. Kern, W. Saenger, A. Zouni and J. Biesiadka, *Nature*, 2005, **438**, 1040; (c) K. N. Ferreira, T. M. Iverson, K. Maghlaoui, J. Barber and S. Iwata, *Science*, 2004, **303**, 1831; (d) J. P. McEvoy and G. W. Brudvig, *Chem. Rev.*, 2006, **106**, 4455; (e) L. M. Utschig and M. C. Thurnauer, *Acc. Chem. Res.*, 2004, **37**, 439.
- 39 (a) G. de la Torre, G. Bottari, M. Sekita, A. Hausmann, D. M. Guldi and T. Torres, *Chem. Soc. Rev.*, 2013, **42**, 8049; (b) *Organic Nanomaterials*, ed. T. Torres and G. Bottari, John Wiley & Sons, Hoboken, NJ, 2013; (c) G. Bottari, G. de la Torre, D. M. Guldi and T. Torres, *Chem. Rev.*, 2010, **110**, 6768.
- 40 (a) O. Ito and F. D'Souza, *Molecules*, 2012, **17**, 5816; (b) F. D'Souza and O. Ito, *Chem. Soc. Rev.*, 2012, **41**, 86; (c) S. Fukuzumi and K. Ohkubo, *Dalton Trans.*, 2013, **42**, 15846.
- 41 K. Ohkubo, K. Mase, E. Karnas, J. L. Sessler and S. Fukuzumi, *J. Phys. Chem. C*, 2014, **118**, 18436.
- 42 (a) M. Valik, V. Král, E. Herdtweck and F. P. Schmidtchen, *New J. Chem.*, 2007, **31**, 703; (b) V. D. Jadhav, E. Herdtweck and F. P. Schmidtchen, *Chem. – Eur. J.*, 2008, **14**, 6098; (c) J. L. Sessler, E. Karnas, S. K. Kim, Z. Ou, M. Zhang, K. M. Kadish, K. Ohkubo and S. Fukuzumi, *J. Am. Chem. Soc.*, 2008, **130**, 15256.
- 43 H.-S. P. Wong and D. Akinwande, *Carbon Nanotube and Graphene Device Physics*, Cambridge University Press, Cambridge, 2010, DOI: 10.1017/CBO9780511778124.
- 44 (a) M.-E. Ragoussi, J. Malig, G. Katsukis, B. Butz, E. Spiecker, G. de la Torre, T. Torres and D. M. Guldi, *Angew. Chem., Int. Ed.*, 2012, **51**, 6421; (b) K. Nikolaos, J. Ortiz, K. Ohkubo, T. Hasobe, S. Fukuzumi, A. Sastre-Santos and N. Tagmatarchis, *J. Phys. Chem. C*, 2012, **116**, 20564.
- 45 M.-E. Ragoussi, G. Katsukis, A. Roth, J. Malig, G. de la Torre, D. M. Guldi and T. Torres, *J. Am. Chem. Soc.*, 2014, **136**, 4593.
- 46 J. Malig, N. Jux, D. Kiessling, J.-J. Cid, P. Vázquez, T. Torres and D. M. Guldi, *Angew. Chem., Int. Ed.*, 2011, **50**, 3561.
- 47 A. Roth, M.-E. Ragoussi, L. Wibmer, G. Katsukis, G. de la Torre, T. Torres and D. M. Guldi, *Chem. Sci.*, 2014, **5**, 3432.
- 48 (a) V. Sgobba and D. M. Guldi, *Chem. Soc. Rev.*, 2009, **38**, 165; (b) A. J. Hilmer, K. Tvrđy, J. Zhang and M. S. Strano, *J. Am. Chem. Soc.*, 2013, **135**, 11901.
- 49 A. Troeger, M. Ledendecker, J. T. Margraf, V. Sgobba, D. M. Guldi, B. F. Vieweg, E. Spiecker, S.-L. Suraru and F. Wuerthner, *Adv. Energy Mater.*, 2012, **2**, 536.
- 50 C. S. Allen, G. Liu, Y. Chen, A. W. Robertson, K. He, Z. Porfyrakis, J. Zhang, G. Briggs, D. Andrew and J. H. Warner, *Nanoscale*, 2014, **6**, 572.
- 51 J. Bartelmess, C. Ehli, J.-J. Cid, M. García-Iglesias, P. Vázquez, T. Torres and D. M. Guldi, *Chem. Sci.*, 2011, **2**, 652.
- 52 J. Bartelmess, C. Ehli, J.-J. Cid, M. García-Iglesias, P. Vázquez, T. Torres and D. M. Guldi, *J. Mater. Chem.*, 2011, **21**, 8014.
- 53 V. Strauss, A. Gallego, G. de la Torre, T. W. Chamberlain, A. N. Khlobystov, T. Torres and D. M. Guldi, *Faraday Discuss.*, 2014, **172**, 61.
- 54 J. Bartelmess, B. Ballesteros, G. de la Torre, D. Kiessling, S. Campidelli, M. Prato, T. Torres and D. M. Guldi, *J. Am. Chem. Soc.*, 2010, **132**, 16202.
- 55 M. Ince, J. Bartelmess, D. Kiessling, K. Dirian, M. V. Martinez-Diaz, T. Torres and D. M. Guldi, *Chem. Sci.*, 2012, **3**, 1472.
- 56 C. G. Claessens, D. Gonzalez-Rodriguez, S. M. Rodriguez-Morgade, A. Medina and T. Torres, *Chem. Rev.*, 2014, **114**, 2192.
- 57 I. Sanchez-Molina, C. G. Claessens, B. Grimm, D. M. Guldi and T. Torres, *Chem. Sci.*, 2013, **4**, 1338.
- 58 I. Sanchez-Molina, B. Grimm, C. Krick, M. Rafael, C. G. Claessens, D. M. Guldi and T. Torres, *J. Am. Chem. Soc.*, 2013, **135**, 10503.
- 59 (a) D. Gonzalez-Rodriguez, T. Torres, M. M. Olgmstead, J. Rivera, M. A. Herranz, L. Echegoyen, C. A. Castellanos and D. M. Guldi, *J. Am. Chem. Soc.*, 2006, **128**, 10680; (b) D. Gonzalez-Rodriguez, E. Carbonell, G. de M. Rojas, C. A. Castellanos, D. M. Guldi and T. Torres, *J. Am. Chem. Soc.*, 2010, **132**, 16488; (c) C. R. Nieto, J. Guilleme, C. Villegas, J. L. Delgado, D. Gonzalez-Rodriguez, N. Martín, T. Torres and D. M. Guldi, *J. Mater. Chem.*, 2011, **21**, 15914; (d) C. Romero-Nieto, J. Guilleme, J. Fernandez-Ariza, S. M. Rodriguez-Morgade, D. Gonzalez-Rodriguez, T. Torres and D. M. Guldi, *Org. Lett.*, 2012, **14**, 5656; (e) L. Feng, M. Rudolf, O. Trukhina, Z. Slanina, F. Uhlik, X. Lu, T. Torres, D. M. Guldi and T. Akasaka, *Chem. Commun.*, 2015, **51**, 330.